Sulfation roasting of nickel oxide-sulfide mixed ore concentrate in the presence of ammonium sulfate

Li, Guangshi; Xiong, Xiaolu; Wang, Liping; Che, Lang; Wei, Lizhen ; Cheng, Hongwei; Zou, Xingli; Xu, Qian; Zhou, Zhongfu; Li, Shenggang; Lu, Xionggang

Published in:
Metals

DOI:
10.3390/met9121256

Publication date:
2019

Citation for published version (APA):
Li, G., Xiong, X., Wang, L., Che, L., Wei, L., Cheng, H., Zou, X., Xu, Q., Zhou, Z., Li, S., & Lu, X. (2019). Sulfation roasting of nickel oxide-sulfide mixed ore concentrate in the presence of ammonium sulfate: experimental and DFT studies. *Metals*, *9*(12), [1256]. https://doi.org/10.3390/met9121256

metals

MDPI

Article

Sulfation Roasting of Nickel Oxide–Sulfide Mixed Ore Concentrate in the Presence of Ammonium Sulfate: Experimental and DFT Studies

Guangshi Li [1], Xiaolu Xiong [1,*], Liping Wang [1], Lang Che [1], Lizhen Wei [1], Hongwei Cheng [1], Xingli Zou [1], Qian Xu [1], Zhongfu Zhou [1,2], Shenggang Li [3,4] and Xionggang Lu [1,3,*]

1 School of Materials Science and Engineering & State Key Laboratory of Advanced Special Steel, Shanghai University, 99 Shangda Road, Shanghai 200444, China; lgs@shu.edu.cn (G.L.); lipingwang1103@foxmail.com (L.W.); chelang7975@shu.edu.cn (L.C.); weilizhen1105@foxmail.com (L.W.); hwcheng@shu.edu.cn (H.C.); xlzou@shu.edu.cn (X.Z.); qianxu@shu.edu.cn (Q.X.); z.zhou@shu.edu.cn (Z.Z.)

2 Department of Physics, Institute of Mathematics, Physics and Computer Science, Aberystwyth University, Aberystwyth SY23 3FL, UK

3 School of Physical Science and Technology, ShanghaiTech University, 393 Middle Huaxia Road, Shanghai 201210, China; lisg@sari.ac.cn

4 Key Laboratory of Low-Carbon Conversion Science and Engineering, Shanghai Advanced Research Institue, Chinese Academy of Sciences, 100 Haike Road, Shanghai 201210, China

* Correspondence: xlxiong@t.shu.edu.cn (X.X.); luxg@shu.edu.cn (X.L.); Tel.: +86-021-9692-8188 (X.X.)

Received: 31 October 2019; Accepted: 22 November 2019; Published: 25 November 2019

Abstract: Sulfation roasting, a common activation technique, is a potential method for cleaner production of nickel from complex low-grade ores. In this study, nickel oxide–sulfide mixed ore concentrate was roasted with the addition of ammonium sulfate under a static air atmosphere, and the roasted products were leached by water, in order to evaluate the extraction of metals. The ammonium sulfate activation roasting was investigated thoroughly and systematically by thermogravimetry–differential scanning calorimetry, X-ray diffraction, and scanning electron microscopy. Particularly, the interface sulfation behavior and path were studied by the density functional theory (DFT) method. The results showed that a large amount of nonferrous metal sulfate (70% Ni, 89% Co, and 90% Cu) was generated, while iron was almost entirely transformed into iron oxide under appropriate roasting conditions of adding ammonium sulfate at a mass ratio of 200%, heating to 650 °C at 10 °C/min, and holding for 120 min. It was found that activation of ammonium sulfate can take two different paths: one in which ammonium sulfate directly reacts with raw ores below 500 °C and the other in which the SO_2 decomposed from sulfates (ammonium sulfate, intermediate ammonium ferric sulfate, and ferric sulfate) reacts with the intermediate metal sulfides (NiS and Cu_2S). The interface sulfation mechanism of NiS and Cu_2S was investigated deeply by DFT method, which showed that there are two paths of sulfation for NiS or Cu_2S, and both of them are thermodynamically favored. Thus, a thorough and systematic investigation of ammonium sulfate activation roasting of nickel oxide–sulfide mixed ore is provided; this might be a potential basis for future industrial applications of ammonium sulfate activation roasting techniques in complex mineral metallurgy.

Keywords: sulfation; roasting; nickel ore; ammonium sulfate; DFT; leaching

1. Introduction

Nickel is a significant strategic metal, and sulfide and oxide ores are the main sources of nickel production around the world. Nickel sulfide minerals have comprised more than half of the resources

for nickel metallurgy for decades. With the gradual consumption of high-grade nickel sulfide mineral resources, oxide ore (laterite) and low-grade nickel oxide–sulfide mixed ore are becoming more and more important in nickel metallurgy [1]. Highly efficient separation of nickel and iron is essential and difficult for the extractive metallurgy of either nickel laterite or nickel-oxide-sulfide mixed ore (NOSMO) [2]. The conventional matte smelting technique, which is famous for its high efficiency in sulfide ore metallurgy, can produce difficulties when processing oxide-based ores [3]. NOSMO is becoming a vitally important mineral resource for nickel production in China [4]. The specific features of nickel ore predetermine the necessity to develop novel pyro- or hydro-metallurgical techniques as alternatives.

To date, researchers have made efforts to develop new metallurgical processes to treat laterite or oxide–sulfide mixed ore; these mainly include selective reduction [5–12] and selective leaching [1,2,13–19]. The selective reduction technique is more suitable for the treatment of nickel laterite, while selective leaching is a more appropriate process for NOSMO. The fundamental concept of selective leaching is to transform nickel oxides or nickel sulfides into water- or acid-soluble phases, while iron and other impurities remain in solid slag [20,21]. In order to obtain higher extraction rates of valuable nonferrous metals, different kinds of chemical additives have been used for activated roasting pretreatment before the selective leaching process [22–24]. Compared to strong corrosive additive media (such as H_2SO_4, Cl_2, and SO_2), salt solid additives (sulfate and chloride) are more environmentally friendly, which might result in potentially cleaner nickel production by using the roasting–leaching technique [21,25,26]. Because the sulfation roasting technique has a unique advantage in the process of nonferrous metal mineral, it has been studied by many researches [27–30]. Several kinds of salt solid additives have been reported as an effective sulfating agent during the roasting of polymetallic sulfide ore, such as sulfide [31], sodium sulfate [32], ferric sulfate [33], and ammonium sulfate [34].

As a potentially more economic and green metallurgical process, ammonium sulfate activation roasting has shown good applicability and has been widely investigated recently [19,20,26,30,35–38]. In particular, Mu et al. developed a low-temperature roasting-water leaching technique to treat complex low-grade nickel ore and achieved high extraction rates of nonferrous metals from raw minerals [19,20,39]. It was found that the gas products generated from ammonium sulfate thermal decomposition include NH_3, SO_2, N_2, and H_2O [40,41]. Therefore, the roasting reaction mechanism might be quite complex due to the variety of reactants. However, most researchers agree that the direct reactions between ammonium sulfate and minerals (metal oxides or sulfides) are mainly responsible for the effective sulfation of metals during the roasting process [2,19,42]. Clearly, there may be some truth to this, but it may be not the whole story of ammonium sulfate during the roasting process. Previous studies showed that the sulfation of nickel remained at a relatively low level after roasting with ammonium sulfate additive alone, but if other chemical media (sodium sulfate, sulfuric acid, etc.) were added, the sulfation yield of nickel reached 90% or more [19,20,39]. Additionally, similar studies have shown that incomplete sulfation of nickel is still exhibited during the roasting process, even after increasing the dosage of ammonium sulfate [2]. Therefore, there remain some ambiguities regarding the reaction mechanism of ammonium sulfate activation roasting of nickel ore, and there is a bottleneck to higher sulfation of nickel. It is necessary to clarify the situation and gain insight into the nature of ammonium sulfate's action in the sulfation of nickel ores.

Recently, density functional theory (DFT) calculations were applied to explore the oxidation of sulfide minerals, which is important for mineral processing and valuable metal extraction [43,44]. In our previous work, DFT calculations were performed successfully to investigate the oxidation mechanisms of chalcopyrite ($CuFeS_2$) and pentlandite ($Fe_{4.5}Ni_{4.5}S_8$) [45,46]. The computational results were in good agreement with our experimental observations [47]. Because the sulfation roasting of sulfides is a controllable oxidation process, DFT might be a suitable and powerful technique to study the behavior and mechanism of ammonium sulfate additives during the roasting process.

As the content of main valuable mineral (pentlandite, chalcopyrite, etc.) in NOSMO is too low to be detected by XRD and other characterizations, a floatation concentrate of NOSMO was used as the

raw materials in this study. The ammonium sulfate activation roasting of NOSMO concentrate was performed on a thermogravimetry–differential scanning calorimeter (TG–DSC) in an air atmosphere. The sulfation roasting-water leaching process is discussed with the evaluation of several parameters, including the roasting temperature, dosage of ammonium sulfate, heating rate, and holding time. The transformation behaviors of the microstructure and crystal phase were characterized by X-ray diffraction (XRD) and scanning electron microscopy (SEM), respectively. Furthermore, we used DFT to explain the sulfation mechanism for NiS and Cu_2S. Considering the atmosphere involved during the experiment, O_2 and SO_2 adsorption were both considered to elucidate the detailed reaction process.

2. Materials and Methods

2.1. Materials

The NOSMO concentrate sample used in this study originated from Jinchuan Group Co., Ltd. (Jinchang, Gansu, China). The concentrate sample was dried at 100 °C for 12 h and then passed through 200 mesh prior to experimentation. Semiquantitative estimation of all elements in this powder sample was investigated by X-ray fluorescence technique (XRF), and accurate quantitative analysis of elements, except O and S, was measured by inductively coupled plasma mass spectrometry (ICP-AES). The results of the chemical analysis of this powder sample are shown in Table 1. The nickel, cobalt, copper, and iron contents were 8.93%, 0.24%, 6.51%, and 28.26%, respectively. The main minerals, which were identified from the X-ray diffraction (XRD) pattern (Figure 1), were pentlandite [$(FeNi)_9S_8$, PDF#73-0515], chalcopyrite ($CuFeS_2$, PDF#83-0983), magnetite (Fe_3O_4, PDF#72-2303), pyrrhotite 4M (Fe_7S_8, PDF#29-0723), pyrite (FeS_2, PDF#71-1680), quartz (SiO_2, PDF#79-1912), willemseite [$(Ni,Mg)_3(Si_2O_5)_2(OH)_2$, PDF#22-0711], and nepouite [$(Ni,Mg)_3Si_2O_5(OH)_4$, PDF#25-0524]. Ammonium sulfate (analytical grade) was purchased from Sinopharm Group Co. Ltd., Shanghai, China, and ground into particles that were passing through 200 mesh before use.

Table 1. Chemical composition of the NOSMO concentrate sample (wt.%).

Fe	O	S	Ni	Mg	Cu	Si	Ca	Al	Co
28.26	22.43	19.61	8.93	6.66	6.51	6.45	0.52	0.39	0.24

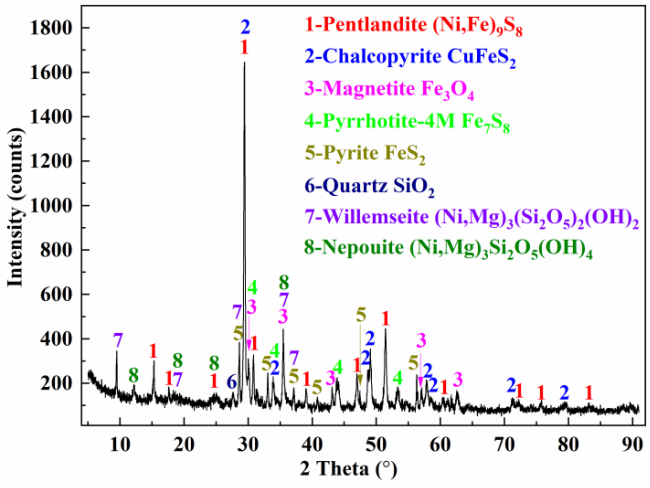

Figure 1. XRD pattern of the NOSMO concentrate sample.

2.2. Experimental Procedure

A quantity of 5 g of the NOSMO concentrate sample was weighed and finely powdered in an agate mortar, and the fine powder of the NOSMO sample mixed well with a desired amount of ground ammonium sulfate (100–200 mesh) in each experiment by using an agate mortar. Then the mixture was

added to a silica crucible. The sample was introduced into the cold furnace and then heated up to target temperature with a certain rate. Sulfation roasting experiments were performed by using a muffle furnace. The roasted products were cooled inside the furnace to room temperature and then leached with hot deionized water (80 °C) with a liquid-to-solid ratio of 4:1 mL/g for 30 min. The leaching slurry was then filtered with a Buchner funnel. The effects of roasting temperature, ammonium sulfate dosage, heating rate, and holding time were studied via the flowsheet shown in Figure 2.

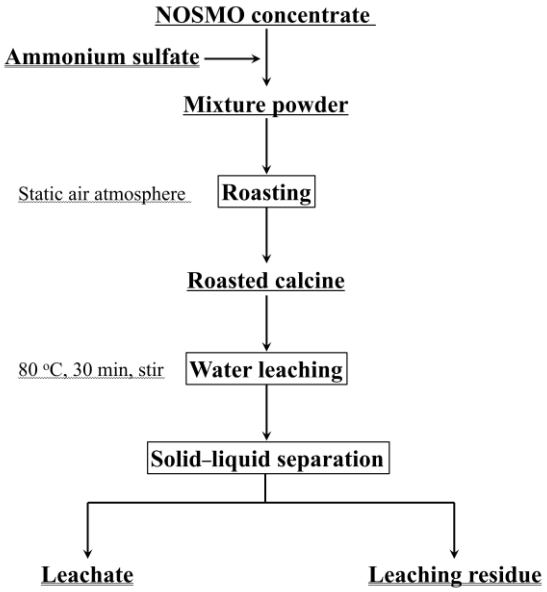

Figure 2. Ammonium sulfate activation roasting-water leaching process flowsheet.

2.3. Characterization Methods

Thermogravimetry–differential scanning calorimetry (TG–DSC) analyses (NETZSCH STA 44 F3 Jupiter, Alden, German) were performed on the NOSMO concentrate sample, ammonium sulfate, and their mixture (mass ratio of 1:2) from 100 to 1000 °C, at a heating rate of 10 °C/min under an air atmosphere (a flow rate of 40 mL/min). A quantity of 20 mg of fine-powder sample was weighed for each TG–DSC test. The ion concentrations of Fe, Co, Ni, and Cu in the leachate were analyzed, using a inductively coupled plasma–atomic emission spectrometer (ICP-AES) (7300 DV, Perkin Elmer, Waltham, MA, USA). The microstructure of the calcine was observed by using a tungsten filament scanning electron microscope (TF-SEM) (SU-1500, HITACHI, Tokyo, Japan). The XRD patterns were measured on an X-ray diffractometer (D8 Advance, Bruker, Billerica, MA, USA), using Cu Kα radiation with a 2θ range of 5°–90°, a step size of 0.02°, and a step time of 1 s.

2.4. Computational Details

DFT calculations were performed as described previously [46,47]. The space group of NiS (millerite) is R3m, and its optimized cell parameters of $a = b = 9.564$ Å and $c = 3.126$ Å are consistent with the experimental data ($a = b = 9.607$ Å, $c = 3.143$ Å) [48]. The p (1 × 2) supercell of the NiS (100) slab containing 24 atoms and including a vacuum layer of 10 Å was employed, where the bottom three of the six atomic layers were fixed. Cu_2S has an orthorhombic cell with space group Abm2 [49]. The p (1 × 2) supercell of the (001) surface for Cu_2S contains six layers with the bottom three fixed.

3. Results and Discussion

3.1. Thermal Analysis of the Roasting Process

The typical thermal analysis curves for NOSMO concentrate mixed with ammonium sulfate, as well as the blank contrast samples (ammonium sulfate and NOSMO concentrate, respectively), are shown in Figure 3. There was no marked change up to 285 °C in the mixture of ammonium sulfate and NOSMO concentrate during the roasting process (Figure 3a). Two well-defined endothermic peaks at 325 and 365 °C, respectively, were observed, and the simultaneous losses in mass were also marked as 25% (named Step 1) and 6% (named Step 2), respectively. This phenomenon is largely attributable to the thermal decomposition of ammonium sulfate, as shown in Figure 3b. However, with the increase in temperature, a small exothermic peak was first observed at 425 °C. This was accompanied by a corresponding increase of mass (7%) in the TG curve. This step (named Step 3) was mainly the combination of the early oxidation of NOSMO concentrate and the further decomposition of ammonium sulfate. The further sulfation reactions (named Step 4) resulted in a mass gain of 2% and exothermal peaks (460 and 530 °C) in the temperature range 450–600 °C. This simultaneous stage also occurred for the nickel concentrate sample shown in Figure 3c, which confirms the formation of metal sulfates. Above 600 °C (named Step 5), a drastic mass loss, as well as endothermic peaks, was observed, as shown in Figure 3a,c. This might be attributed to the decomposition of metal sulfates.

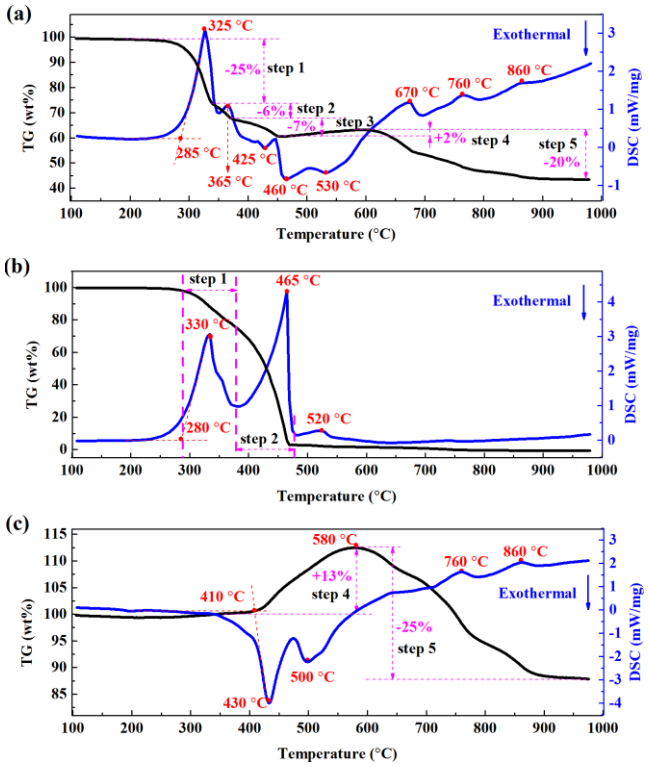

Figure 3. TG–DSC curves of a mixture of ammonium sulfate and NOSMO concentrate (**a**), ammonium sulfate alone (**b**), and NOSMO concentrate alone (**c**).

3.2. Effect of Roasting Temperature

The effect of the sulfation roasting temperature on the recovery of metal species by water leaching was first investigated. For each test, a mixture of 5 g of NOSMO concentrate sample and 10 g of ammonium sulfate was heated to different temperatures at 20 °C/min and maintained for 2 h in static air. The water-leaching results of the roasted products are presented in Figure 4. As can be seen, the leaching yields of nonferrous metals (Cu, Ni, and Co) increased substantially with a rise in the

roasting temperature, peaked at around 650 °C, and then decreased sharply when the temperature continued to rise. This is because a higher temperature may facilitate sulfation reactions between nonferrous metal sulfides and ammonium sulfate in the range 300–650 °C, under an air atmosphere. The decomposition of these sulfates ($CuSO_4$, $NiSO_4$, and $CoSO_4$) contributes mainly to the descent of the nonferrous metal extraction. Similarly, the iron leaching recovery slightly increased at first and then decreased with the rising temperature. When the temperature reached 600 °C, the extraction of Fe gradually approached zero. As revealed in Figure 4, there was an optimum roasting temperature in the range 600–650 °C, at which we can achieve considerable extraction of nonferrous metals (~9% Cu, ~79% Co, and 59% Ni) and complete iron separation (~0.1% Fe); thus, this process may be used to separate and extract nonferrous metals from NOSMO.

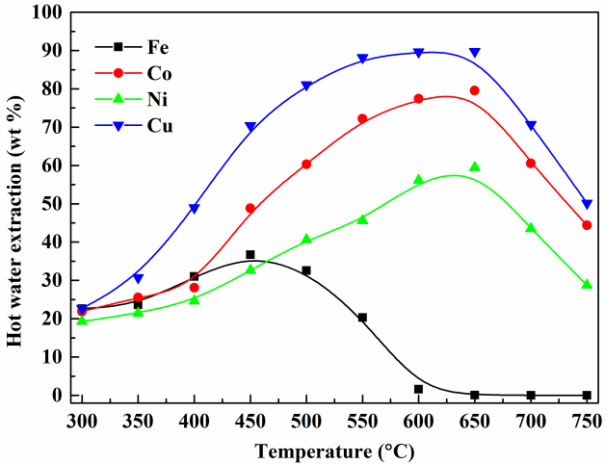

Figure 4. Effect of roasting temperature on the leaching recovery of metals.

3.3. Effect of the Addition of Ammonium Sulfate

As an essential factor, the dosage of ammonium sulfate was investigated for its effect on the sulfation of valuable metals. A mixture of 5 g of NOSMO concentrate sample and a selected amount of ammonium sulfate was heated to 650 °C at 20 °C/min and held for 2 h in static air. The leaching efficiency is plotted against the weight percentage of ammonium sulfate to NOSMO concentrate in Figure 5. It can be seen that the dosage of ammonium sulfate had a significant effect on nonferrous metals. The extraction of Ni was substantially promoted from 30% to 60%, with increasing ammonium sulfate addition. The extraction of Cu and Co were also improved to a certain degree. However, because iron sulfates cannot stay stable at around 650 °C, the dosage of ammonium sulfate had little or no influence over the leaching efficiency of iron. Therefore, the optimum dosage of ammonium sulfate would be double the mass of NOSMO concentrate, and this dosage was consequently chosen for the subsequent experiments.

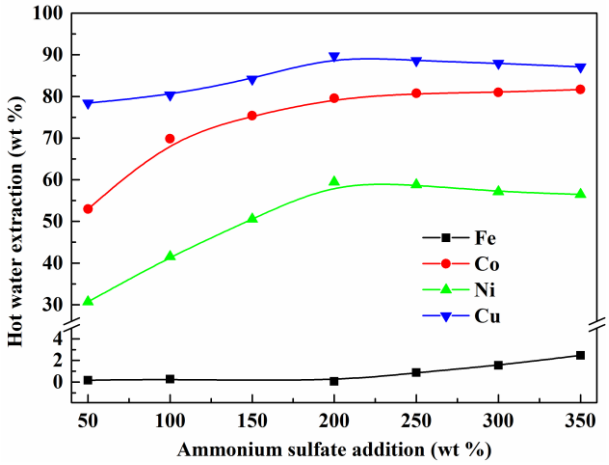

Figure 5. Effect of the dosage of ammonium sulfate on the leaching recovery of metals.

3.4. Effect of Heating Rate

Roasting experiments were conducted under different heating rates, in order to understand the effect of the heating process on the sulfation of the nonferrous metals. In these experiments, a mixture of 5 g NOSMO concentrate sample and 10 g ammonium sulfate was heated to 650 °C and held for 2 h under an air atmosphere. The hot-water extraction of valuable metals (Fe, Co, Ni, and Cu) is shown in Figure 6. The heating rate significantly influenced the leaching yields of nonferrous metals. As demonstrated in Figure 6, the recovery of nonferrous metals showed slight increases with the increasing heating rate in the range from 1 to 10 °C/min. However, the leaching yields started to decline sharply when the heating rate reached 10 °C/min. It is obvious that an overly rapid heating rate may inhibit the sulfation of nonferrous metals and result in low leaching efficiency of nonferrous metals. Indeed, this is due to incomplete sulfation reactions, which are attributed to the rapid decomposition of ammonium sulfate. Our previous work also reported that the heating rate significantly influenced the sulfation of nickel sulfides [21]. Additionally, with the increasing heating rate, the amount of appreciable dissolution of iron decreased gradually from 4% to almost zero. As a result, the optimum sulfation roasting heating rate was 10 °C/min in this experiment, which was adopted for further investigations.

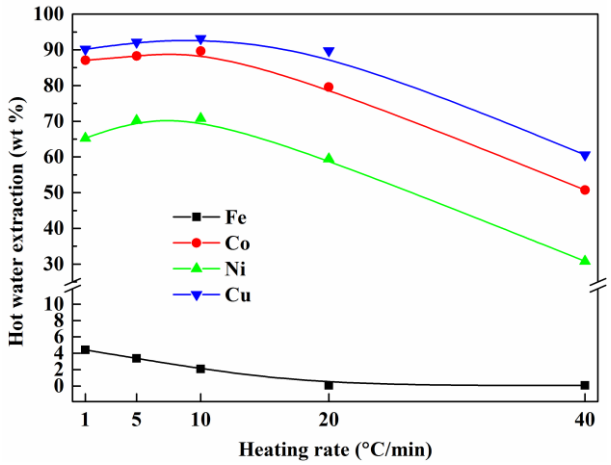

Figure 6. Effect of heating rate during roasting on the leaching recovery of metals.

3.5. Effect of Holding Time

To study the effect of holding time on the sulfation of NOSMO concentrate, mixtures of 5 g NOSMO samples and 10 g of ammonium sulfate were heated to 650 °C at 10 °C/min and held for 30 to 180 min.

The results of the hot-water extraction of valuable metals (Fe, Co, Ni, and Cu) are plotted in Figure 7. With the increasing holding time, the leaching yields of Ni, Co, and Cu gradually increased and then remained at a certain level at 120 min. More specifically, the extraction of Ni, Co, and Cu reached 70%, 89%, and 90%, respectively, while the extraction of Fe was about 2%. Thus, under appropriate roasting conditions (added ammonium sulfate with a mass ratio of 200%, heated to 650 °C at 10 °C/min and held for 120 min), a large amount of nonferrous metal sulfate was formed, while the iron was almost completely turned into iron oxide. Thus, excellent separation of the nonferrous metals and iron was achieved by the water leaching process.

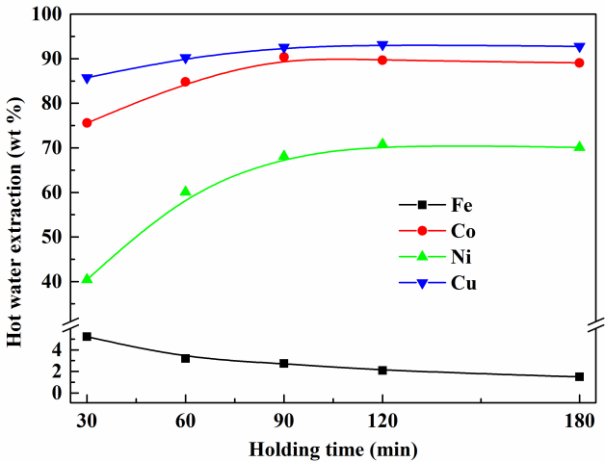

Figure 7. Effect of holding time during roasting on the leaching recovery of metals.

3.6. The Transformation Behaviors of the Crystal Phase and Microstructure of Roasting Products

Recently, studies of the sulfation roasting of nickel sulfides in air revealed strong additive-dependent behavior [19,21,39]. In order to gain insight into the sulfation roasting process, the microscopic morphology and crystal structure of the roasting products were investigated thoroughly and systematically by XRD (Figure 8) and SEM (Figure 9), respectively, which was conducive to analysis of the behavior of ammonium sulfate and to deducing the reaction mechanism of ammonium sulfate roasting.

As shown in Figure 8a, the product roasted at 450 °C mainly consisted of $NH_4Fe(SO_4)_2$, $Fe_2(SO_4)_3$, $CuSO_4$, $NiSO_4$, $MgSO_4$, $CuFeS_2$, Cu_2S, NiS, Ni_3S_4, $(Ni,Mg)_3(Si_2O_5)_2(OH)_2$, and SiO_2. First, ammonium sulfate was gradually decomposed into a gas mixture (SO_2, NH_3, N_2, SO_2, and H_2O). The thermal decomposition stages can be represented by Equations (1)–(3) [41]:

$$(NH_4)_2SO_4 = NH_4HSO_4 + NH_3 \quad (1)$$

$$2NH_4HSO_4 = (NH_4)_2S_2O_7 + H_2O \quad (2)$$

$$3(NH_4)_2S_2O_7 = 2NH_3 + 2N_2 + 6SO_2 + 9H_2O \quad (3)$$

Meanwhile, ammonium sulfate reacted with metal sulfides in the presence of O_2. The corresponding chemical reactions can be summarized as follows [20]:

$$4Fe_7S_8 + 54(NH_4)_2SO_4 + 69O_2 = 28(NH_4)_3Fe(SO_4)_3 + 24NH_3 + 14H_2O + 2SO_2 \quad (4)$$

$$4CuFeS_2 + 22(NH_4)_2SO_4 + 17O_2 = 4(NH_4)_3Fe(SO_4)_3 + 4CuSO_4 + 4NH_3 + 2H_2O \quad (5)$$

$$8(Ni,Fe)_9S_8 + 112(NH_4)_2SO_4 + 93O_2 = 36NiSO_4 + 36(NH_4)_3Fe(SO_4)_3 + 58NH_3 + 29H_2O \quad (6)$$

$$2FeS_2 + 3(NH_4)_2SO_4 + 7O_2 = 2(NH_4)_3Fe(SO_4)_3 + 2SO_2 \quad (7)$$

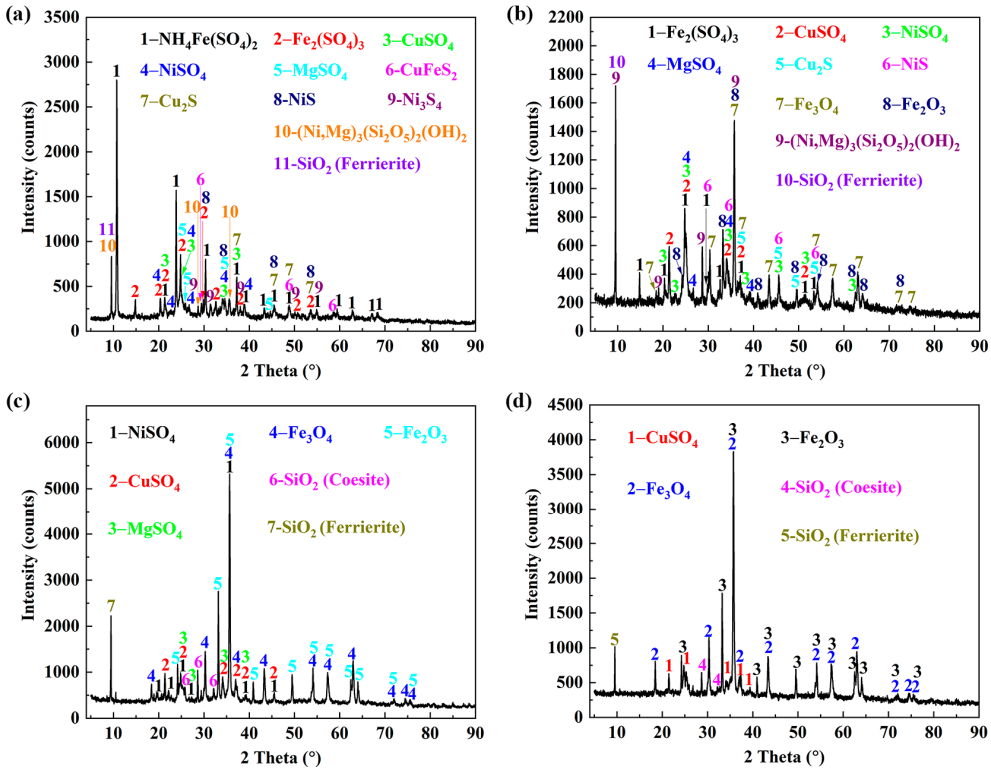

Figure 8. The XRD phase identification of roasted products at different temperatures (adding mass ratio of ammonium sulfate to NOSMO concentrate sample: 200%, heating rate: 10 °C/min, holding time: 2 h): (**a**) 450 °C, (**b**) 550 °C, (**c**) 650 °C, and (**d**) 750 °C.

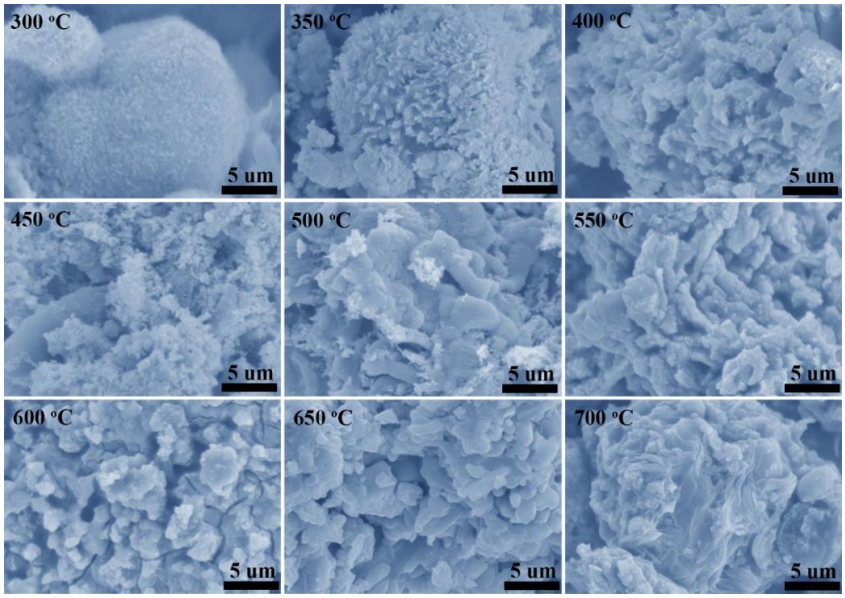

Figure 9. Effect of temperatures on the micromorphology of roasted products (static air atmosphere, addition of 200% ammonium sulfate, heating at 10 °C/min, and holding for 2 h at each temperature).

As shown in Equations (4) and (7), ammonium sulfate can react with iron sulfides to produce SO_2 gas, and the intermediate ammonium ferric sulfate ($(NH_4)_3Fe(SO_4)_3$) can be decomposed further to generate SO_3 gas by Equation (8) [40]:

$$2(NH_4)_3Fe(SO_4)_3 = Fe_2(SO_4)_3 + 4NH_3 + 2SO_3 + 3H_2O \quad (8)$$

Additionally, polymetallic sulfides can be decomposed into monometallic sulfides, for instance, Cu_2S, NiS, and Ni_3S_4. This has been systematically studied and proved by previous work [47], and the reaction equations were deduced and shown as follows:

$$2CuFeS_2 + 6O_2 = Cu_2S + Fe_2(SO_4)_3 \quad (9)$$

$$8(Ni,Fe)_9S_8 + 51O_2 + 38SO_3 = 12Ni_3S_4 + 18Fe_2(SO_4)_3 \quad (10)$$

$$Ni_3S_4 + O_2 = 3NiS + SO_2 \quad (11)$$

Particularly, the $(Ni,Mg)_3Si_2O_5(OH)_4$ disappeared at 450 °C, while $(Ni,Mg)_3(Si_2O_5)_2(OH)_2$ remained. It is suggested that $(Ni,Mg)_3Si_2O_5(OH)_4$ may have reacted with $(NH_4)_3Fe(SO_4)_3$, as illustrated by Equation (12):

$$2(Ni,Mg)_3Si_2O_5(OH)_4 + 6(NH_4)_2SO_4 = 3NiSO_4 + 3MgSO_4 + 4SiO_2 + 12NH_3 + 10H_2O \quad (12)$$

Based on Equations (1)–(8), we conclude that the direct reaction between ammonium sulfate and metal sulfides can result in the formation of intermediate ammonium ferric sulfate and SO_2 gas. Because the decomposition temperature of $(NH_4)_3Fe(SO_4)_3$ might be higher than that of pure ammonium sulfate, there may be a higher concentration of SO_2/SO_3 gas on further sulfation interface. For that reason, the sulfation of nickel and copper can be improved by ammonium sulfate activation roasting. In addition, the oxidation of metal sulfides could also occur in this process, and the reaction paths were studied and presented in our previous work [39].

As the temperature increased to 550 °C, the roasting product mainly consisted of $Fe_2(SO_4)_3$, $CuSO_4$, $NiSO_4$, $MgSO_4$, Cu_2S, NiS, Fe_3O_4, Fe_2O_3, $(Ni,Mg)_3(Si_2O_5)_2(OH)_2$, and SiO_2 (Figure 8b). The decomposition of $(NH_4)_3Fe(SO_4)_3$ and $Fe_2(SO_4)_3$ during this process may result in increasing Fe_2O_3 and SO_2, and, thus, higher pressure of SO_2 on the reaction interface could accelerate the sulfation of nickel and copper sulfides. This shows good agreement with the water leaching results in Figure 4. When the temperature increased to 650 °C (Figure 8c), the NiS was turned into $NiSO_4$ and $NiFe_2O_4$ (or NiO), while Cu_2S was almost entirely transformed into $CuSO_4$. This means that the sulfation of nickel sulfide is more difficult than that of copper sulfide. Meanwhile, the $(Ni,Mg)_3Si_2O_5(OH)_4$ disappeared at 650 °C (Figure 8c). This finding can be explained by the possibility that $Fe_2(SO_4)_3$ can react with $(Ni,Mg)_3Si_2O_5(OH)_4$, as illustrated by Equation (13):

$$2(Ni,Mg)_3Si_2O_5(OH)_4 + 2Fe_2(SO_4)_3 = 3NiSO_4 + 3MgSO_4 + 2Fe_2O_3 + 4SiO_2 + 4H_2O \quad (13)$$

However, the peaks of $NiSO_4$ and $MgSO_4$ were not detected in Figure 8d when the roasting temperature further increased to 750 °C. This may be attributed to the decomposition of sulfates at a higher temperature. Combined with Figures 4 and 8d, it can be concluded that the sulfation of nickel and copper sulfide can be suppressed by excessive temperature. For that reason, the sulfation temperature should be kept at 650 °C or below.

As demonstrated in Figure 9, the SEM images of the roasted products show great diversity among different temperatures, ranging from 300 to 700 °C. The surface of the roasted product was characterized by floccules at 300 °C, which is attributed to the decomposition of the ammonium sulfate additive. When the roasting temperature increased to 500 °C, the flocculent-shaped surface appearance gradually faded away. This result shows excellent agreement with the TG–DSC test in Figure 3. As the roasting temperature rose to the range between 500 and 650 °C, the roasted products gradually became loose and porous. This is owing to inner diffusion of O_2 and outer release of SO_2/SO_3 during inner oxidation of the sulfide ore particles. When the roasting temperature was above 700 °C, the surface of the roasted products presented a characterization of a molten sintering state (Figure 9). It may be that large amounts of eutectic sulfates ($CuSO_4$ and $NiSO_4$) formed at a higher roasting temperature (≥700 °C).

3.7. The Sulfation Mechanism for the NiS and Cu_2S Surfaces by DFT Studies

As mentioned, ammonium sulfate can promote the sulfation of nickel and copper by direct reaction and SO_2 gas decomposition. The indirect reaction plays a significant role in the sulfation of NiS and Cu_2S, both of which are the intermediate products during the NOSMO roasting process. Thus, in an effort to increase our understanding of the sulfation route and behavior, DFT was used to calculate the interaction between O_2/SO_2 and metal sulfide intermediates.

As shown in Figure 10, the (100) surface of NiS was adopted to investigate the sulfation mechanism. The (100) slab of NiS contains five layers, with the bottom two layers fixed and the top three layers relaxed. After the optimization of the clean surface, the oxygen dissociative adsorption on the NiS (100) surface was studied, as shown in Figure 10c. The two oxygen atoms bind with two nickel atoms, leading to an adsorption energy of −1.81 eV. The adsorbed oxygen atoms provide the sites for SO_2 interaction. The interaction between SO_2 and the NiS (100) surface via two paths was studied; these are clearly shown in Figure 10c. In Path 1, SO_2 binds with only one adsorbed oxygen atom with an S–O bond length of 1.59 Å, resulting in a thermodynamically more stable structure with adsorption energy of −0.75 eV. Based on the formed SO_3^{2-}, the desorption of SO_3 was further explored. The SO_3 desorption leads the relative energy to be more positive by 1.26 eV, implying that this process is exothermic. In addition, the adsorption energy of SO_3 on the adsorbed oxygen atom of the NiS (100) surface was predicted to be −3.23 eV, finally leading to the formation of SO_4^{2-}. In Path 2, SO_2 directly interacts with two oxygen atoms, leading to the formation of SO_4^{2-} directly.

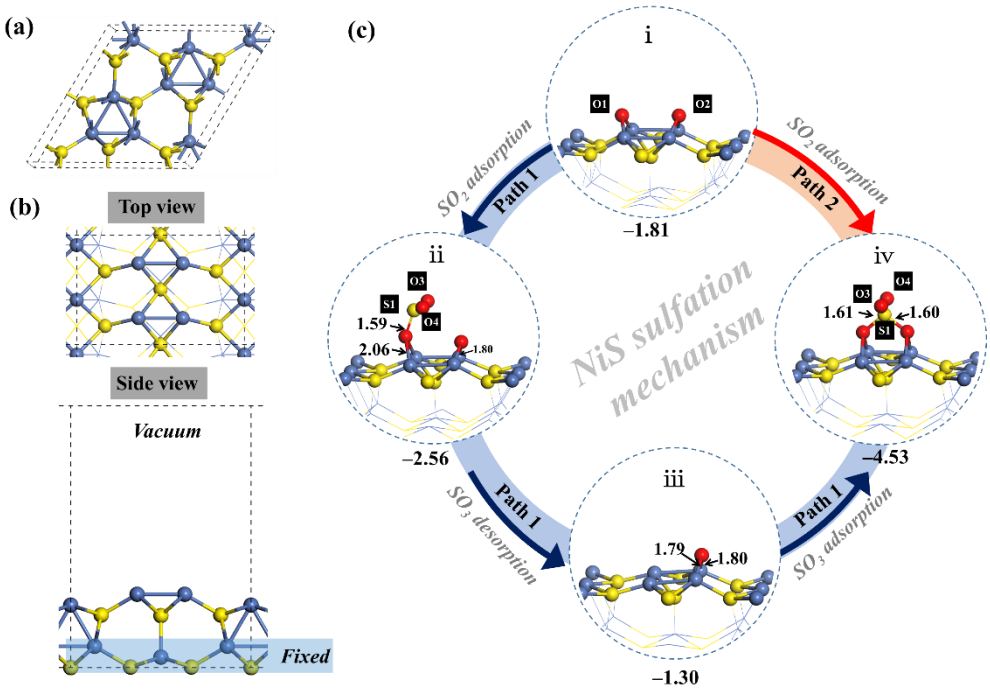

Figure 10. (**a**) Bulk structure of NiS. (**b**) The (100) surface of NiS (the top image represents the top view, and the bottom image represents the side view of the NiS (100) surface). (**c**) Sulfation mechanism for the NiS (100) surface.

The sulfation mechanism of Cu_2S was also investigated through O_2 and SO_2 adsorption on the (001) surface of Cu_2S. Figure 11b,c shows the top view and the side view of the (001) surface of Cu_2S, respectively, showing that the copper atoms of the first layer are all equivalent and the bottom three layers are fixed. After the relaxation, oxygen dissociation on the (001) surface of Cu_2S leads to an adsorption energy of −1.09 eV with a Cu–O bond length of 1.81 Å. Similar to the sulfation process of NiS, the sulfation mechanism of Cu_2S was also elucidated in two paths. In Path 1, the SO_2 interacts

with the Cu_2S surface through the adsorbed oxygen atom, leading to an adsorption energy drop of −0.77 eV, with an S–O bond length of 1.58 Å. When the adsorbed species of SO_2 and the adsorbed oxygen atom desorb simultaneously from the Cu_2S (001) surface, the adsorption energy becomes more positive, indicating that this process is also exothermic. Eventually, the SO_3 adsorption leads to the formation of the SO_4^{2-} species on the Cu_2S (001) surface. In Path 2, when the SO_2 directly interacts with the two adsorbed oxygen atoms, SO_4^{2-} can also be formed successfully.

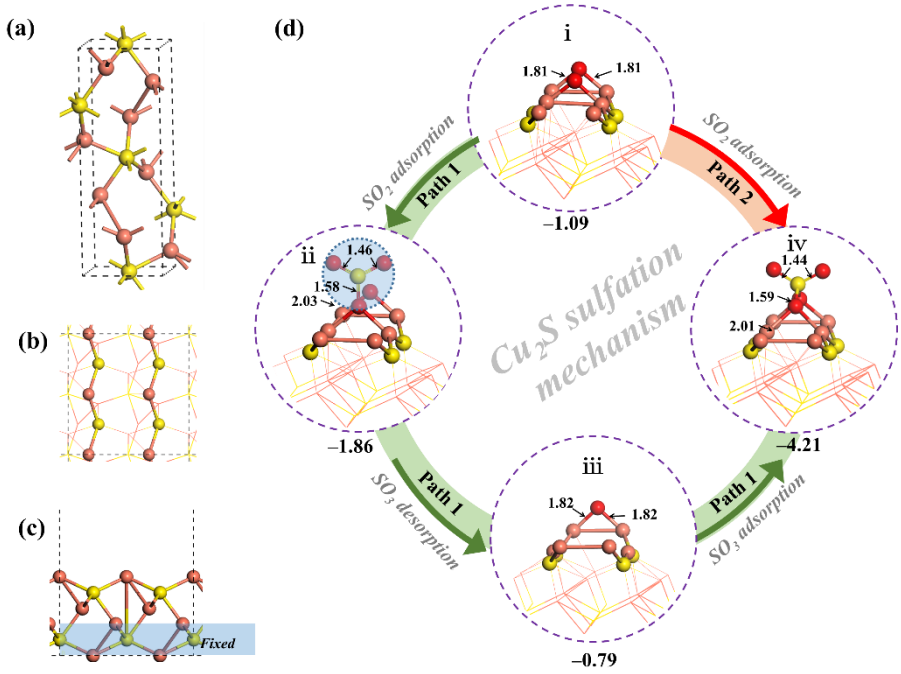

Figure 11. (**a**) Bulk structure of Cu_2S. (**b**) Top view and (**c**) side view of the (001) surface of Cu_2S. (**d**) Sulfation mechanism for the Cu_2S (001) surface.

4. Conclusions

Ammonium sulfate activation roasting-water leaching was studied as a suitable and green technique to extract nonferrous metals from NOSMO concentrate. The TG–DSC tests indicated that the decomposition of ammonium sulfate and sulfation of NOSMO concentrate was consistent in terms of the temperature range. The effects of several parameters, including the roasting temperature, dosage of ammonium sulfate additive, heating rate, and holding time, were investigated by the control variable method. The results demonstrated that 70% Ni, 89% Co, 90% Cu, and 2% Fe were recovered under appropriate conditions (adding ammonium sulfate at a mass ratio of 200%, heating to 650 °C at 10 °C/min, and holding for 120 min). It was found that ammonium sulfate cannot only directly react with metal sulfides at a lower roasting temperature but can also promote the sulfation of metal sulfides by increasing the interface partial pressure of SO_2 at a higher temperature. This increase in SO_2 can be attributed to the decomposition of ammonium sulfate and intermediate ammonium ferric sulfate. In addition, DFT calculations were performed, focusing on the respective detailed sulfation mechanisms of NiS and Cu_2S. Based on our calculation results, sulfation of both NiS and Cu_2S can be achieved by the interaction between O_2 and SO_2. When the SO_2 directly interacts with two oxygen atoms, sulfation can be achieved directly. Besides this, sulfation can also be promoted by the formation of SO_3 species. It is concluded that both paths can promote the sulfation of NiS and Cu_2S, which are both thermodynamically favored.

Author Contributions: G.L., X.X., and X.L. conceived of and designed the experiments; G.L. performed the experiments and analyzed the data; X.X. and S.L. conducted the DFT calculations; L.W. (Liping Wang), L.C., and L.W. (Lizhen Wei) participated in the roasting and leaching experiments; H.C., Q.X., X.Z., and Z.Z. contributed reagents/materials/analysis tools; G.L. and X.X. wrote this paper.

Funding: This work was financially supported by the China Postdoctoral Science Foundation, the Super Postdoctoral Incentive Program in Shanghai, the Steel Joint Research Foundation of National Natural Science Foundation of China–China Baowu Iron and Steel Group Co. Ltd. (Grant No. U1860203), the National Natural Science Foundation of China (Grant No. 51576164), National Basic Research Program of China (973 Program) (Grant 2014CB643403), and the CAS Interdisciplinary Innovation Team.

Conflicts of Interest: The authors declare no conflict of interest.

References

1. Li, G.; Zhou, Q.; Zhu, Z.; Luo, J.; Rao, M.; Peng, Z.; Jiang, T. Selective leaching of nickel and cobalt from limonitic laterite using phosphoric acid: An alternative for value-added processing of laterite. *J. Clean. Prod.* **2018**, *189*, 620–626. [CrossRef]
2. Li, J.; Li, D.; Xu, Z.; Liao, C.; Liu, Y.; Zhong, B. Selective leaching of valuable metals from laterite nickel ore with ammonium chloride-hydrochloric acid solution. *J. Clean. Prod.* **2018**, *179*, 24–30. [CrossRef]
3. Klyushnikov, A.M. Sulphuric-acid leaching of ural oxidized nickel ore with sodium sulfite and fluoride additives. *J. Min. Sci.* **2018**, *54*, 141–146. [CrossRef]
4. Zeng, X.; Xu, M.; Li, J. Examining the sustainability of China's nickel supply: 1950–2050. *Resour. Conserv. Recycl.* **2018**, *139*, 188–193. [CrossRef]
5. Yang, J.; Zhang, G.; Ostrovski, O.; Jahanshahi, S. Selective reduction of an Australian garnieritic laterite ore. *Miner. Eng.* **2019**, *131*, 79–89. [CrossRef]
6. Rao, M.; Li, G.; Zhang, X.; Luo, J.; Peng, Z.; Jiang, T. Reductive roasting of nickel laterite ore with sodium sulfate for Fe-Ni production. Part I: Reduction/sulfidation characteristics. *Sep. Sci. Technol.* **2016**, *51*, 1408–1420. [CrossRef]
7. Cui, Y.; Zhang, G.; Jahanshahi, S.; Ostrovski, O. Carbonylation of nickel and selectively reduced laterite ore. *J. S. Afr. Inst. Min. Metall.* **2018**, *118*. [CrossRef]
8. Zhu, D.; Pan, L.; Guo, Z.; Pan, J.; Zhang, F. Utilization of limonitic nickel laterite to produce ferronickel concentrate by the selective reduction-magnetic separation process. *Adv. Powder Technol.* **2019**, *30*, 451–460. [CrossRef]
9. Wang, X.-P.; Sun, T.-C.; Chen, C.; Kou, J. Effects of Na_2SO_4 on iron and nickel reduction in a high-iron and low-nickel laterite ore. *Int. J. Miner. Metall. Mater.* **2018**, *25*, 383–390. [CrossRef]
10. Rodrigues, F.; Pickles, C.; Peacey, J.; Elliott, R.; Forster, J. Factors affecting the upgrading of a nickeliferous limonitic laterite ore by reduction roasting, thermal growth and magnetic separation. *Minerals* **2017**, *7*, 176. [CrossRef]
11. Pickles, C.A.; Elliott, R. Thermodynamic analysis of selective reduction of nickeliferous limonitic laterite ore by carbon monoxide. *Miner. Process. Extr. Metall.* **2015**, *124*, 208–216. [CrossRef]
12. Gao, L.; Liu, Z.; Pan, Y.; Ge, Y.; Feng, C.; Chu, M.; Tang, J. Separation and recovery of iron and nickel from low-grade laterite nickel ore using reduction roasting at Rotary Kiln followed by magnetic separation technique. *Min. Metall. Explor.* **2018**, *36*, 375–384. [CrossRef]
13. Zhang, P.; Guo, Q.; Wei, G.; Meng, L.; Han, L.; Qu, J.; Qi, T. Extraction of metals from saprolitic laterite ore through pressure hydrochloric-acid selective leaching. *Hydrometallurgy* **2015**, *157*, 149–158. [CrossRef]
14. Chang, Y.; Zhao, K.; Pesic, B. Selective leaching of nickel from prereduced limonitic laterite under moderate HPAL conditions—Part I: Dissolution. *J. Min. Metall. Sect. B Metall.* **2016**, *52*, 127–134. [CrossRef]
15. Zhang, P.; Guo, Q.; Wei, G.; Meng, L.; Han, L.; Qu, J.; Qi, T. Leaching metals from saprolitic laterite ore using a ferric chloride solution. *J. Clean. Prod.* **2016**, *112*, 3531–3539. [CrossRef]
16. Kobayashi, H.; Shoji, H.; Asano, S.; Imamura, M. Selective nickel leaching from nickel and cobalt mixed sulfide using sulfuric acid. *Mater. Trans.* **2018**, *59*, 1458–1464. [CrossRef]
17. Luo, J.; Li, G.; Rao, M.; Peng, Z.; Zhang, Y.; Jiang, T. Atmospheric leaching characteristics of nickel and iron in limonitic laterite with sulfuric acid in the presence of sodium sulfite. *Miner. Eng.* **2015**, *78*, 38–44. [CrossRef]
18. Oxley, A.; Smith, M.E.; Caceres, O. Why heap leach nickel laterites? *Miner. Eng.* **2016**, *88*, 53–60. [CrossRef]

19. Mu, W.; Huang, Z.; Xin, H.; Luo, S.; Zhai, Y.; Xu, Q. Extraction of copper and nickel from low-grade nickel sulfide ore by low-temperature roasting, selective decomposition and water-leaching process. *JOM* **2019**. [CrossRef]
20. Mu, W.; Cui, F.; Huang, Z.; Zhai, Y.; Xu, Q.; Luo, S. Synchronous extraction of nickel and copper from a mixed oxide-sulfide nickel ore in a low-temperature roasting system. *J. Clean. Prod.* **2018**, *177*, 371–377. [CrossRef]
21. Li, G.; Cheng, H.; Chen, S.; Lu, X.; Xu, Q.; Lu, C. Mechanism of Na_2SO_4 promoting nickel extraction from sulfide concentrates by sulfation roasting–water leaching. *Metall. Mater. Trans. B* **2018**, *49*, 1136–1148. [CrossRef]
22. Mukherjee, T.K.; Menon, P.R.; Shukla, P.P.; Gupta, C.K. Chloridizing roasting process for a complex Sulfide concentrate. *JOM* **1985**, *37*, 29–33. [CrossRef]
23. Swamy, Y.V.; Kar, B.B.; Mohanty, J.K. Physico-chemical characterization and sulphatization roasting of low-grade nickeliferous laterites. *Hydrometallurgy* **2003**, *69*, 89–98. [CrossRef]
24. Yu, D.; Utigard, T.A.; Barati, M. Fluidized bed selective oxidation-sulfation roasting of nickel sulfide concentrate: Part II. sulfation roasting. *Metall. Mater. Trans. B* **2013**, *45*, 662–674. [CrossRef]
25. Xu, C.; Cheng, H.; Li, G.; Lu, C.; Lu, X.; Zou, X.; Xu, Q. Extraction of metals from complex sulfide nickel concentrates by low-temperature chlorination roasting and water leaching. *Int. J. Miner. Metall. Mater.* **2017**, *24*, 377–385. [CrossRef]
26. Cui, F.; Mu, W.; Wang, S.; Xin, H.; Xu, Q.; Zhai, Y. A sustainable and selective roasting and water-leaching process to simultaneously extract valuable metals from low-grade Ni-Cu matte. *JOM* **2018**, *70*, 1977–1984. [CrossRef]
27. Guo, X.; Li, D.; Park, K.-H.; Tian, Q.; Wu, Z. Leaching behavior of metals from a limonitic nickel laterite using a sulfation–roasting–leaching process. *Hydrometallurgy* **2009**, *99*, 144–150. [CrossRef]
28. Prasad, S.; Pandey, B.D. Alternative processes for treatment of chalcopyrite—A review. *Miner. Eng.* **1998**, *11*, 763–781. [CrossRef]
29. Ingraham, T.R.; Kerby, R. Roasting in extractive metallurgy a thermodynamic and kinetic review. *Can. Metall. Q.* **1967**, *6*, 89–119. [CrossRef]
30. Theys, L.F.; Lee, L.V. Sulfate roasting copper-cobalt sulfide concentrates. *JOM* **1958**, *10*, 134–136. [CrossRef]
31. Tümen, F.; Bailey, N.T. Recovery of metal values from copper smelter slags by roasting with pyrite. *Hydrometallurgy* **1990**, *25*, 317–328. [CrossRef]
32. Fletcher, A.; Shelef, M. The role of alkali sulfates in promoting the sulphation roasting of nickel sulfides. *Unit Process Hydrometall.* **1964**, *24*, 946–970.
33. Altundoğan, H.S.; Tümen, F. Metal recovery from copper converter slag by roasting with ferric sulphate. *Hydrometallurgy* **1997**, *44*, 261–267. [CrossRef]
34. Sukla, L.B.; Panda, S.C.; Jena, P.K. Recovery of cobalt, nickel and copper from converter slag through roasting with ammonium sulphate and sulphuric acid. *Hydrometallurgy* **1986**, *16*, 153–165. [CrossRef]
35. Yang, Z.; Li, Y.; Lou, Q.; Liu, D.; Ning, Y.; Yang, S.; Tang, Y.; Zhang, Y.; Tang, Z.; Wang, X. Release of uranium and other trace elements from coal ash by $(NH_4)_2SO_4$ activation of amorphous phase. *Fuel* **2019**, *239*, 774–785. [CrossRef]
36. Zhou, Y.; Yang, H.; Xue, X.-X.; Yuan, S. Separation and recovery of iron and rare earth from Bayan Obo tailings by magnetizing roasting and $(NH_4)_2SO_4$ activation roasting. *Metals* **2017**, *7*, 195. [CrossRef]
37. Liu, W.; Wang, X.; Lu, Z.; Yue, H.; Liang, B.; Lü, L.; Li, C. Preparation of synthetic rutile via selective sulfation of ilmenite with $(NH_4)_2SO_4$ followed by targeted removal of impurities. *Chin. J. Chem. Eng.* **2017**, *25*, 821–828. [CrossRef]
38. Shao, H.-M.; Shen, X.-Y.; Sun, Y.; Liu, Y.; Zhai, Y.-C. Reaction condition optimization and kinetic investigation of roasting zinc oxide ore using $(NH_4)_2SO_4$. *Int. J. Miner. Metall. Mater.* **2016**, *23*, 1133–1140. [CrossRef]
39. Cui, F.; Mu, W.; Wang, S.; Xin, H.; Xu, Q.; Zhai, Y.; Luo, S. Sodium sulfate activation mechanism on co-sulfating roasting to nickel-copper sulfide concentrate in metal extractions, microtopography and kinetics. *Miner. Eng.* **2018**, *123*, 104–116. [CrossRef]
40. Li, Y.; Liu, H.; Peng, B.; Min, X.; Hu, M.; Peng, N.; Yuang, Y.; Lei, J. Study on separating of zinc and iron from zinc leaching residues by roasting with ammonium sulphate. *Hydrometallurgy* **2015**, *158*, 42–48. [CrossRef]
41. Halstead, W.D. Thermal decomposition of ammonium sulphate. *J. Appl. Chem.* **2007**, *20*, 129–132. [CrossRef]
42. Liu, X.; Feng, Y.; Li, H.; Yang, Z.; Cai, Z. Recovery of valuable metals from a low-grade nickel ore using an ammonium sulfate roasting-leaching process. *Int. J. Miner. Metall. Mater.* **2012**, *19*, 377–383. [CrossRef]

43. Mkhonto, P.; Chauke, H.; Ngoepe, P. Ab initio studies of O_2 adsorption on (110) nickel-rich pentlandite ($Fe_4Ni_5S_8$) mineral surface. *Minerals* **2015**, *5*, 665–678. [CrossRef]
44. Sit, P.H.; Cohen, M.H.; Selloni, A. Interaction of oxygen and water with the (100) surface of pyrite: mechanism of sulfur oxidation. *J. Phys. Chem. Lett.* **2012**, *3*, 2409–2414. [CrossRef] [PubMed]
45. Xiong, X.; Hua, X.; Zheng, Y.; Lu, X.; Li, S.; Cheng, H.; Xu, Q. Oxidation mechanism of chalcopyrite revealed by X-ray photoelectron spectroscopy and first principles studies. *Appl. Surf. Sci.* **2018**, *427*, 233–241. [CrossRef]
46. Xiong, X.; Lu, X.; Li, G.; Cheng, H.; Xu, Q.; Li, S. Energy dispersive spectrometry and first principles studies on the oxidation of pentlandite. *Phys. Chem. Chem. Phys.* **2018**, *20*, 12791–12798. [CrossRef]
47. Li, G.; Cheng, H.; Xiong, X.; Lu, X.; Xu, C.; Lu, C.; Zou, X.; Xu, Q. In-situ XRD and EDS method study on the oxidation behaviour of Ni-Cu sulphide ore. *Sci. Rep.* **2017**, *7*, 3212. [CrossRef]
48. Rajamani, V.T.; Prewitt, C. The crystal structure of millerite. *Can. Mineral.* **1974**, *12*, 253–257.
49. Chen, J.; Long, X.; Zhao, C.; Kang, D.; Guo, J. DFT calculation on relaxation and electronic structure of sulfide minerals surfaces in presence of H_2O molecule. *J. Cent. S. Univ.* **2014**, *21*, 3945–3954. [CrossRef]